

# Generalization characteristics of complex-valued reservoir computing for interferometric synthetic aperture radar applications

Bungo Konishi\*, Akira Hirose\* and Ryo Natsuaki\*

\* The University of Tokyo, Tokyo, Japan

E-mail: b.konishi@eis.t.u-tokyo.ac.jp, ahirose@ee.t.u-tokyo.ac.jp, natsuaki@ee.t.u-tokyo.ac.jp

**Abstract**—This paper discusses the principles and properties of complex-valued reservoir computing (CVRC), a proposed method for adaptive processing of interferograms with low computational cost. The topographic information of elevation, slope and aspect, obtained from InSAR data, can be utilized for hazard mapping and land use planning. Many recent studies use convolutional neural networks (CNNs) for image recognition tasks. However, CNNs have problems of high computational cost and resolution degradation of classification results. CVRC, a reservoir computing-based approach, provides a solution to these problems. We compare between CVRC and real-imaginary parts separated reservoir computing, and show that CVRC has a high generalization ability through an experiment on aspect classification.

## I. INTRODUCTION

Synthetic aperture radar (SAR) is a remote sensing technology that observes ground surface with high resolution by synthesizing radar echoes. In particular, the interferogram obtained by interferometric SAR (InSAR) analysis, which uses two SAR data of the same point at two different timings, includes topographic features such as elevation, aspect angle and slope angle. These features are important for hazard mapping and land use planning[1], [2]. In order to utilize radar echo signals, SAR applications must be able to handle complex-valued information, which is a unique feature compared to applications for optical imageries.

Many recent studies have used convolutional neural networks (CNNs), a type of deep neural networks, for image recognition[3]. CNNs have also been widely utilized in SAR data [4], [5], [6], [7], [8]. However, CNNs require high computational cost due to having multiple convolution layers. In addition, CNNs cause resolution degradation of classification results due to the pooling process. To solve these problems, we proposed complex-valued reservoir computing (CVRC) and demonstrated that CVRC has a higher accuracy and a lower computational cost than complex-valued CNNs [8], [9], [10].

Complex numbers can be regarded as two-dimensional information with amplitude-phase or real-imaginary parts. Assuming that the real and imaginary parts are independent, we are able to implement the real-imaginary type by using traditional methods for real numbers. On the other hand, the amplitude-phase type, having information of different qualities each other, must be implemented in a way that handles

complex numbers directly. We implement and compare these two types of reservoir computing-based methods.

The purpose of this paper is to reveal the classification performance and process of CVRC by comparison between CVRC and real-imaginary separated reservoir computing (RVRC)[11], [12]. The experimental results of aspect classification show that CVRC has a higher generalization ability than RVRC.

## II. RESERVOIR COMPUTING

### A. Amplitude-phase complex-valued reservoir computing

Fig. 1 shows the network structure of complex-valued reservoir computing. The network has three layers, an input layer, a hidden layer called reservoir and an output layer. The complex vectors  $\mathbf{u}_t$ ,  $\mathbf{x}_t$  and  $\mathbf{y}_t$  are the input signals, the internal states of the reservoir and the internal states of the output layer, respectively. The weights  $\mathbf{W}_{in}$ ,  $\mathbf{W}_{res}$  and  $\mathbf{W}_{out}$  are complex matrices and the bias  $\mathbf{b}_{out}$  is a complex vector.  $N_{in}$ ,  $N_{res}$  and  $N_{out}$  are the number of neurons in the input layer, the reservoir and the output layer, respectively. The continuous-time dynamics of CVRC is defined as

$$\mathbf{z} = \mathbf{W}_{in}\mathbf{u} + \mathbf{W}_{res}\mathbf{x}, \tag{1}$$

$$\frac{d\mathbf{x}}{dt} = C(-a\mathbf{x} + \tanh(|\mathbf{z}|) \circ \exp(j \arg(\mathbf{z}))) \tag{2}$$

$$\mathbf{y} = \mathbf{W}_{out}\mathbf{x} + \mathbf{b}_{out}. \tag{3}$$

$C$  is the time constant,  $a$  is a leaking decay rate,  $\circ$  is the Hadamard product and both  $\tanh(\cdot)$  and  $\arg(\cdot)$  are applied element-wise. These dynamics can be discretized as

$$\mathbf{z}_t = \mathbf{W}_{in}\mathbf{u}_t + \mathbf{W}_{res}\mathbf{x}_{t-1}, \tag{4}$$

$$\mathbf{x}_t = (1 - \delta C a)\mathbf{x}_{t-1} + \delta C \tanh(|\mathbf{z}_t|) \circ \exp(j \arg(\mathbf{z}_t)), \tag{5}$$

$$\mathbf{y}_t = \mathbf{W}_{out}\mathbf{x}_t + \mathbf{b}_{out}. \tag{6}$$

where  $\delta$  is a discrete interval. To reduce the number of hyperparameters, (5) can be expressed as

$$\mathbf{x}_t = (1 - c)\mathbf{x}_{t-1} + c \tanh(|\mathbf{z}_t|) \circ \exp(j \arg(\mathbf{z}_t)) \tag{7}$$

where  $c$  is a discrete global dynamic speed.

In order to deal with InSAR data appropriately, CVRC treats the complex-valued signals input to the reservoir in a way that is independent of phase reference. We defined two types of activation functions, one for amplitude and one for phase, in

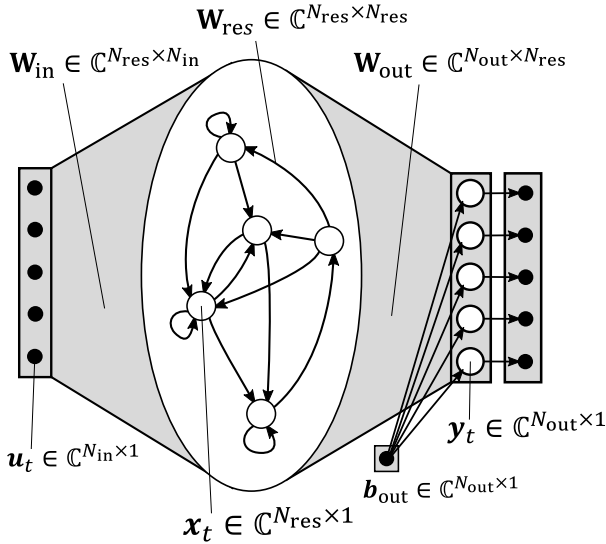


Fig. 1: Structure of amplitude–phase complex-valued reservoir computing

the dynamics of (2), (5) and (7). The activation function for amplitude uses  $\tanh(\cdot)$  to represent the energy saturation. The one for phase represents the rotation of the signals by using the identity function.

We learn only  $\mathbf{W}_{\text{out}}$  and  $\mathbf{b}_{\text{out}}$  connected to the output layer. A static reservoir, having multiple neurons, plays a significant roll in pattern memorization and separation. Since  $\mathbf{y}$  is obtained by a linear combination in (3) and (6),  $\mathbf{W}_{\text{out}}$  and  $\mathbf{b}_{\text{out}}$  are calculated by Tikhonov Regularization as

$$[\mathbf{W}_{\text{out}} \quad \mathbf{b}_{\text{out}}] = ((\mathbf{X}^* \mathbf{X} + \lambda \mathbf{I})^{-1} \mathbf{X}^* \mathbf{D})^T. \quad (8)$$

where  $\lambda$  is a regularization parameter, and  $\mathbf{X}$  and  $\mathbf{D}$  represent an output matrix of all the reservoirs used for training and their corresponding teacher signal matrix, respectively.

### B. Real–imaginary separated reservoir computing

As a conventional implementation, we applied real-valued reservoir computing (RVRC) to an interferogram by separating the real and imaginary parts. The structure of the RVRC network is shown in Fig. 2.

The continuous-time dynamics of RVRC is represented as

$$\frac{d\mathbf{x}}{dt} = C(-a\mathbf{x} + \tanh(\mathbf{W}_{\text{in}}\mathbf{u} + \mathbf{W}_{\text{res}}\mathbf{x})) \quad (9)$$

$$\mathbf{y} = \mathbf{W}_{\text{out}}\mathbf{x} + \mathbf{b}_{\text{out}}. \quad (10)$$

The dynamics is discretized as

$$\mathbf{x}_t = (1 - \delta C a)\mathbf{x}_{t-1} + \delta C \tanh(\mathbf{W}_{\text{in}}\mathbf{u}_t + \mathbf{W}_{\text{res}}\mathbf{x}_{t-1}), \quad (11)$$

$$\mathbf{y}_t = \mathbf{W}_{\text{out}}\mathbf{x}_t + \mathbf{b}_{\text{out}}. \quad (12)$$

To reduce the number of parameters, we simplify (12) as

$$\mathbf{x}_t = (1 - c)\mathbf{x}_{t-1} + c \tanh(\mathbf{W}_{\text{in}}\mathbf{u}_t + \mathbf{W}_{\text{res}}\mathbf{x}_{t-1}) \quad (13)$$

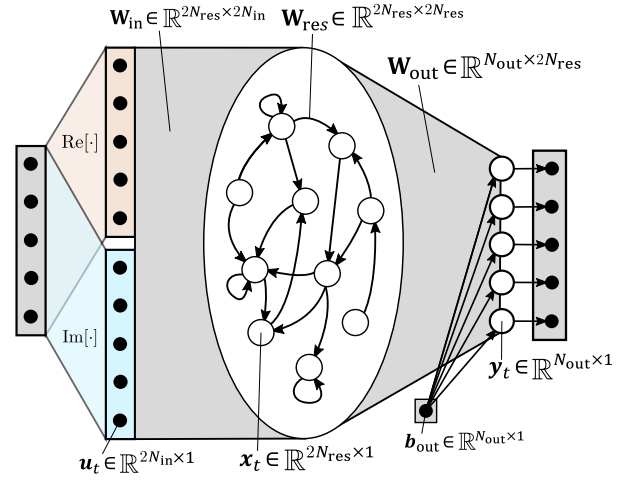


Fig. 2: Structure of real–imaginary parts separated real-valued reservoir computing

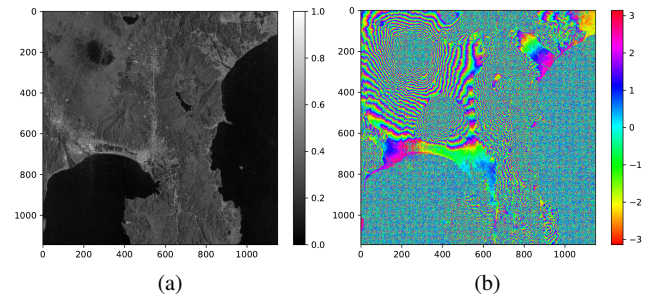


Fig. 3: Original complex interferogram data : (a) amplitude and (b) phase images around Mt. Fuji

RVRC requires twice the number of input terminals as CVRC because it deals with amplitude and phase signals independently. Since all the weights of RVRC are composed of real values, the number of neurons in the reservoir is also twice as that of CVRC. We use (8) to learn  $\mathbf{W}_{\text{out}}$  and  $\mathbf{b}_{\text{out}}$ .

## III. SIGNIFICANCE OF AMPLITUDE–PHASE COMPLEX-VALUED RESERVOIR COMPUTING

### A. Experiment on aspect classification

We conducted an experiment to classify land forms into aspect angles by using CVRC and RVRC. We used the interferogram obtained from two the Advanced Land Observing Satellite (ALOS) data of the Japan Aerospace Exploration Agency (JAXA) around Mt. Fuji, Japan, as shown in Fig. 3. The aspects is defined as four types of slopes (north, west, south and east directions) and a flat plane. The learning and estimation procedures are the same as those for the aspect classification performed in [9] and [10]. Table I shows the hyperparameters of the CVRC and RVRC networks.

Fig. 4 shows the classification results in the whole area by using (a) CVRC, (b) RVRC as well as (c) the ground truth. The classification result of RVRC is not as good as that of CVRC, especially in the flat plane. Fig. 5 shows the classification

TABLE I: Hyperparameters for CVRC and RVRC networks in the experiment on aspect classification

Parameter	Value
The number of neurons in the input layer	$N_{in}$ 5
The number of neurons in the reservoir	$N_{res}$ 5
The number of neurons in the output layer	$N_{out}$ 5
Desireble spectral radius	$\sigma_d$ 0.10
Discrete global dynamic speed	$c$ 0.45
Regularization parameter	$\lambda$ $10^{-12}$

TABLE II: Comparison of accuracy between CVRC and RVRC

	Accuracy [%]				Overall
	Flat	Periphery of Lake Ashi	Mt. Ashitaka	Mt. Ashitaka (west-ridge)	
CVRC	<b>93.1</b>	<b>56.2</b>	<b>48.6</b>	<b>65.6</b>	<b>64.3</b>
RVRC	17.8	50.4	40.7	60.8	57.0

results in the flat area by using (a) CVRC, (b) RVRC as well as (c) the ground truth. RVRC fails to classify the flat plane. Since the amplitude of the flat plane is larger than that of the other areas, the amplitude information is more information rather than the phase information. RVRC is unable to capture the features of flat plane well because it deals with the real and imaginary parts separately. Fig. 6 shows the classification results in a west ridge of Mt. Ashitaka area by using (a) CVRC, (b) RVRC as well as (c) the ground truth. In this area consisted of small ridges, the phase information is more important than the amplitude information to classify it into the aspect angles. CVRC presents a better results with less noise than RVRC.

We show the accuracy of CVRC and RVRC in Table II. CVRC classified land forms with higher accuracy compared with RVRC in all areas. This indicates that CVRC has a high generalization ability.

B. Analysis of the signals in the reservoir

We reveal the classification process by visualizing the signals in the reservoir of CVRC and RVRC. Fig. 7 shows (a) amplitude and (b) phase of the signals in the reservoir of CVRC, and (c) the signals in the reservoir of RVRC in the scanning of the area from the west slope passing the summit to the east slope of Mt. Fuji. Although the phase values of CVRC around the summit of Mt. Fuji are unstable, but those between east and west slopes are clearly different. RVRC is difficult to classify land forms into the two slopes because there are only small differences in the magnitude of the signals.

Fig. 8 shows (a) amplitude and (b) phase of the signals in the reservoir of CVRC, and (c) the signals in the reservoir of RVRC in scanning of the area from the north slope to the south slope of Mt. Fuji. This analysis shows the same trends as Fig. 7.

IV. CONCLUSION

In this paper, we described the dynamics and characteristics of amplitude–phase complex-valued reservoir computing and real–imaginary separated reservoir computing. We conducted

aspect classification and analyzed the signals in the reservoir by using CVRC and RVRC. CVRC classifies land forms with higher accuracies in all areas compared to RVRC and has a high generalization ability.

ACKNOWLEDGEMENT

The authors thank Gouhei Tanaka, Project Associate Professor, International Research Center for Neurointelligence (IRCIN), the University of Tokyo, and Ryosho Nakane, Project Associate Professor, Department of Electrical Engineering and Information Systems, the University of Tokyo, for their advice on experimental design.

A part of this work was supported by JSPS KAKENHI under Grant 18H04105 and also by Cooperative Research Project Program of the Research Institute of Electrical Communication (RIEC), Tohoku University. The Advanced Land Observing Satellite (ALOS) original data are copyrighted by the Japan Aerospace Exploration Agency (JAXA) and provided under JAXA Fourth ALOS Research Announcement PI No. 1154 (AH).

REFERENCES

- [1] Vincenzo Marsala, Alberto Galli, Giorgio Paglia, and Enrico Miccadei. Landslide susceptibility assessment of mauritius island (indian ocean). *Geosciences*, Vol. 9, No. 12, p. 493, 2019.
- [2] E Cevik and Tamer Topal. Gis-based landslide susceptibility mapping for a problematic segment of the natural gas pipeline, hendek (turkey). *Environmental geology*, Vol. 44, No. 8, pp. 949–962, 2003.
- [3] Xujing Yao, Xinyue Wang, Shui-Hua Wang, and Yu-Dong Zhang. A comprehensive survey on convolutional neural network in medical image analysis. *Multimedia Tools and Applications*, pp. 1–45, 2020.
- [4] Xiaoxiang Zhu, Sina Montazeri, Mohsin Ali, Yuansheng Hua, Yuanyan Wang, Lichao Mou, Yilei Shi, Feng Xu, and Richard Bamler. Deep learning meets sar: concepts, models, pitfalls, and perspectives. *IEEE Geoscience and Remote Sensing Magazine*, 2021.
- [5] Zhao Lin, Kefeng Ji, Miao Kang, Xiangguang Leng, and Huanxin Zou. Deep convolutional highway unit network for SAR target classification with limited labeled training data. *IEEE Geoscience and Remote Sensing Letters*, Vol. 14, No. 7, pp. 1091–1095, 2017.
- [6] Yu Zhou, Haipeng Wang, Feng Xu, and Ya-Qiu Jin. Polarimetric SAR image classification using deep convolutional neural networks. *IEEE Geoscience and Remote Sensing Letters*, Vol. 13, No. 12, pp. 1935–1939, 2016.
- [7] Jun Ding, Bo Chen, Hongwei Liu, and Mengyuan Huang. Convolutional neural network with data augmentation for SAR target recognition. *IEEE Geoscience and Remote Sensing Letters*, Vol. 13, No. 3, pp. 364–368, 2016.
- [8] Yuki Sunaga, Ryo Natsuaki, and Akira Hirose. Land form classification and similar land-shape discovery by using complex-valued convolutional neural networks. *IEEE Transactions on Geoscience and Remote Sensing*, Vol. 57, No. 10, pp. 1–11, 2019.
- [9] Bungo Konishi, Akira Hirose, and Ryo Natsuaki. Complex-valued reservoir computing for interferometric sar applications with low computational cost and high resolution. *IEEE Journal of Selected Topics in Applied Earth Observations and Remote Sensing*, Vol. 14, pp. 7981–7993, 2021.
- [10] Bungo Konishi, Akira Hirose, and Ryo Natsuaki. Proposal of complex-valued reservoir computing for topographic aspect classification. In *IEEE International Geoscience and Remote Sensing Symposium 2021*, TH1.O-15.3.
- [11] Herbert Jaeger. The “echo state” approach to analysing and training recurrent neural networks-with an erratum note. *Bonn, Germany: German National Research Center for Information Technology GMD Technical Report 148*, 2001.
- [12] Herbert Jaeger, Mantas Lukoševičius, Dan Popovici, and Udo Siewert. Optimization and applications of echo state networks with leaky-integrator neurons. *Neural networks*, Vol. 20, No. 3, pp. 335–352, 2007.

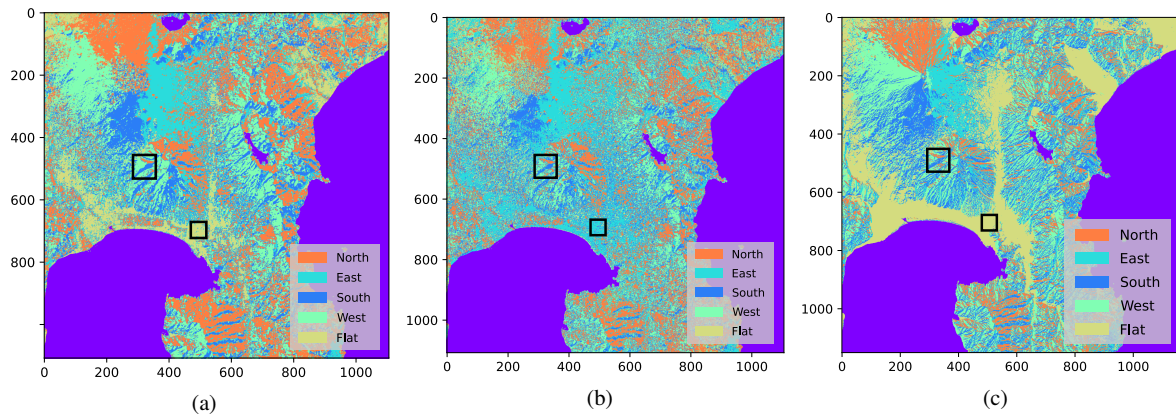


Fig. 4: Classification results in whole area by using (a) CVRC and (b) RVRC as well as (c) ground truth.

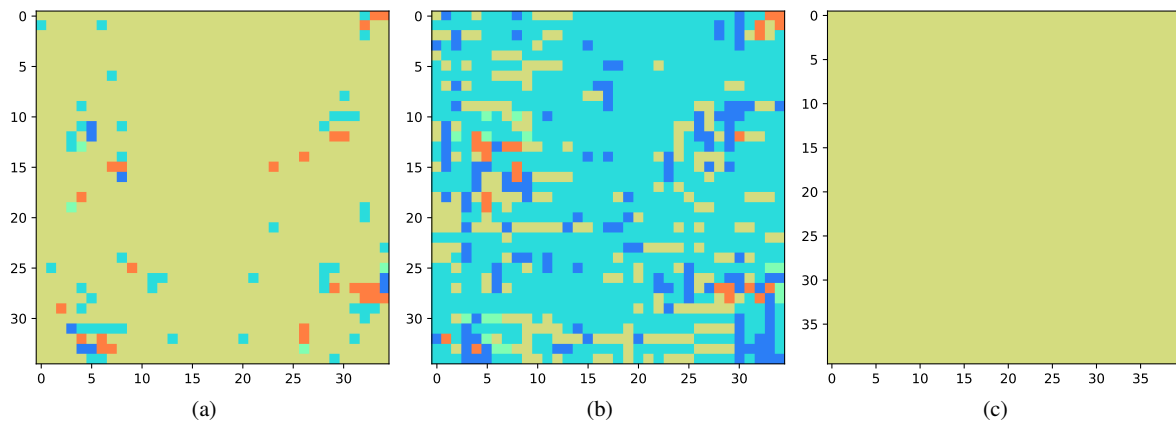


Fig. 5: Classification results in flat plane by using (a) CVRC and (b) RVRC as well as (c) ground truth.

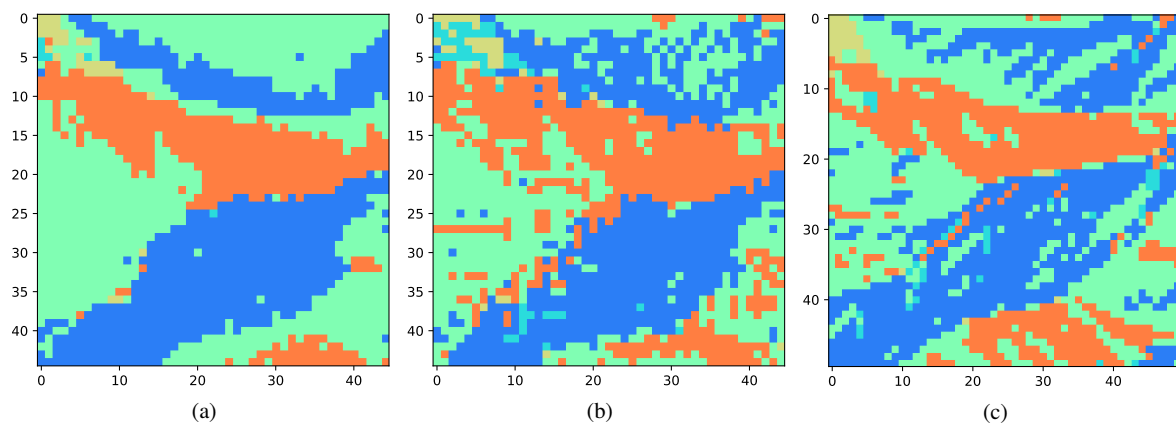


Fig. 6: Classification results in a west ridge of Mt. Ashitaka by using (a) CVRC and (b) RVRC as well as (c) ground truth.

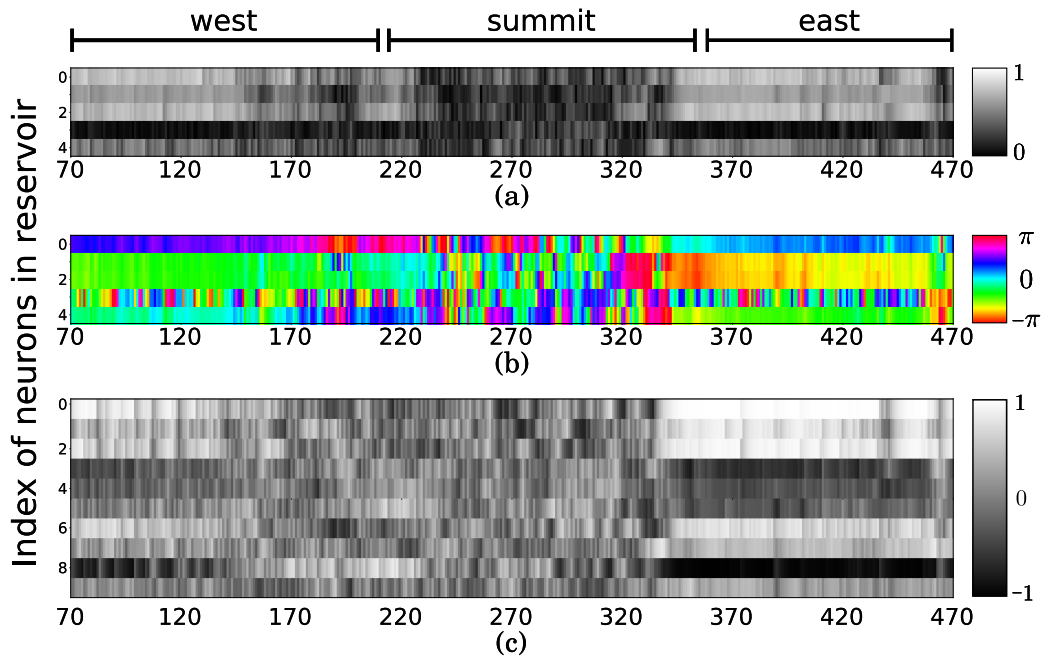


Fig. 7: (a) Amplitude and (b) phase of the signals in the reservoir of CVRC, and (c) the signals in the reservoir of RVRC in scanning of the area from the west slope passing the summit to the east slope of Mt. Fuji.

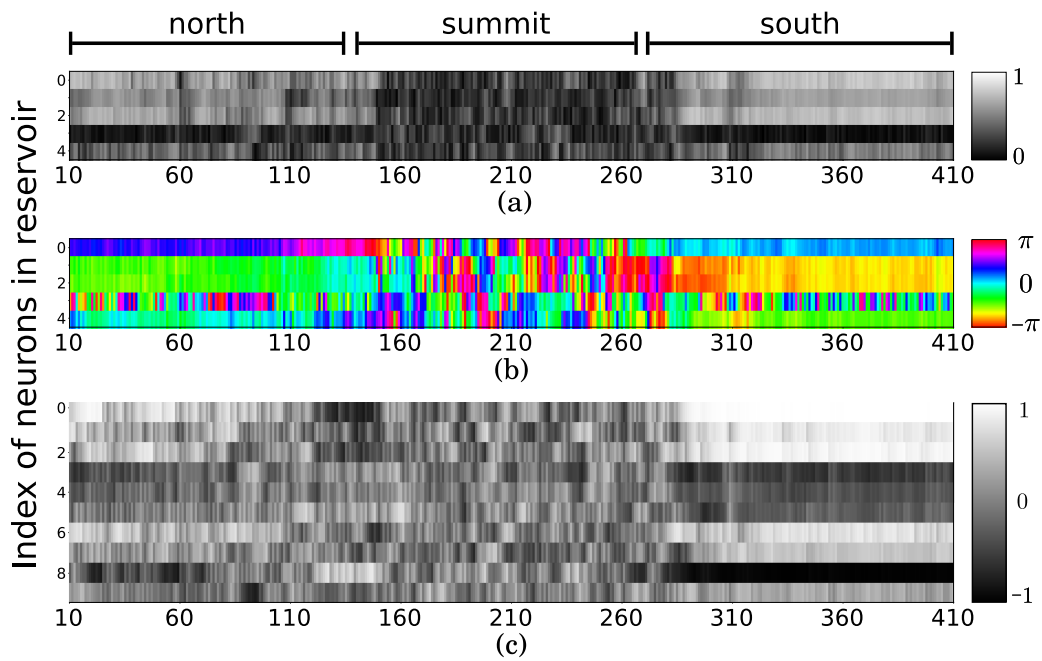


Fig. 8: (a) Amplitude and (b) phase of the signals in the reservoir of CVRC, and (c) the signals in the reservoir of RVRC in scanning of the area from the north slope passing the summit to the south slope of Mt. Fuji.